A New CDMA-Concept using Hybrid Modulation with Noncoherent Detection

Karl-Dirk KAMMEYER and Dirk NIKOLAI

Univ. of Bremen, Dept. of Telecommunications[1], P.O. Box 33 04 40, D-28334 Bremen, Germany
Tel.: ++(49)-421/218-2453, Fax: ++(49)-421/218-3341, E-mail: nikolai@comm.uni-bremen.de

Abstract[2]: In this paper, we present a novel transmission scheme with application to Direct Sequence Code Division Multiple Access (DS-CDMA) combining M-ary orthogonal and PSK modulation. With this "hybrid" modulation procedure, additional data is transmitted in the phase of each M-ary symbol. Note that it is due to *real* valued symbols that this transmission capacity is lost in state-of-the-art communication systems. The bit error probability is derived for both PSK and DPSK as the additional modulation type for an AWGN channel. The analytical results are confirmed by simulations. Finally, we show that the hybrid scheme is applicable to the noncoherent reverse link of the American IS-95 system by introducing an additional DQPSK.

1 Introduction

CONVENTIONAL M-ary modulation schemes such as M-ASK (M-ary amplitude-shift keying) or M-PSK (phase-shift keying) are defined by their complex signal space representation. With the use of direct sequence spread spectrum techniques (DS-SS) it is possible to perform an *encoding in time division*. Here, the source symbols to be transmitted are multiplied by a high rate pseudo-noise (PN) code anyway to facilitate the multiple access. This inherent increase in sampling rate can be used partly to generate distinguishable signals: each group of $\log_2(M)$ binary digits chooses one of M corresponding M-dimensional signal waveforms which differ in shape over time. An *orthogonal* M-ary modulation scheme is obtained when using the Walsh-Hadamard set for the signal waveforms. Such a modulation concept is successfully employed for mobile communications in the uplink of the QUALCOMM CDMA-system (IS-95). Due to the orthogonality, a noncoherent demodulation procedure (Rake receiver with square-law combining) can be used.

The novel hybrid modulation procedure is obtained by combining M_1-ary Walsh encoding with a conventional M_2-ary phase-shift keying (PSK). That means, each Walsh symbol undergoes a phase shift which is determined by the corresponding M_2-PSK symbol; the phase shift is constant for the symbol duration. Due to the constant envelope of the PSK modulation, the Walsh symbols are not further influenced by the phase modulation so they can still be detected noncoherently. With the use of *differential* PSK (DPSK) also the hybrid scheme becomes noncoherent.

We will start with a general description of the hybrid modulation procedure and its application to CDMA. This will provide us with the necessary insight into the idea of hybrid modulation. In section 3, the bit error rate performance for transmission over both AWGN and Rayleigh fading channels is investigated. One key issue of this paper is the derivation of analytical results for the bit error probability. To underline the accuracy, the analytical results are compared with simulations results.

[1]Compressed postscript files of our publications are readily available over Internet at `http://www.comm.uni-bremen.de`.

[2]This work is supported by the German National Science Foundation (DFG-contract # Ka 841/4).

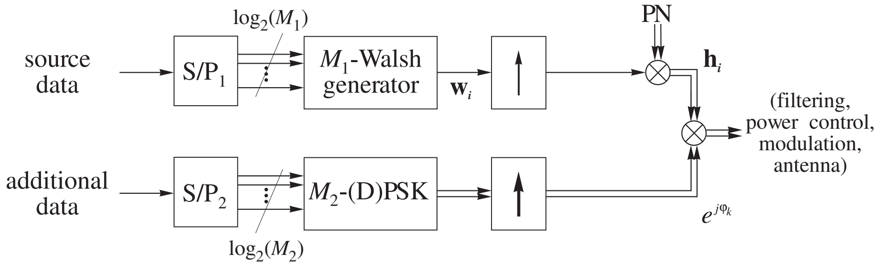

Figure 1: Hybrid modulation scheme

2 Hybrid Modulation

For convenience, we consider the transmission of a single Walsh symbol. The symbol to be transmitted is assumed to a be real valued, orthogonal vector

$$\mathbf{w_j^T} = (w_j(0), \dots, w_j(N_s - 1)) \ ,$$

$$\mathbf{w_i}^* \mathbf{w_j} = N_s \delta_{ij} \ ,$$

with components $w_j(k) \in \{-1, 1\}$. Such a binary vector can be generated from Walsh functions, also known as Hadamard matrices. That means, $\log_2(M_1)$ binary digits choose one of M_1 corresponding Walsh symbols. In the uplink of the IS-95 system [1], the M_1-ary Walsh symbols with $M_1 = 64$ are spread by a factor of 4 due to the multiplication with a complex pseudo-random noise (PN) binary code $\mathrm{P}_u(k)$ to yield the transmission symbol

$$\mathbf{h_i} = \mathbf{P}_u \, \mathbf{w_i}$$

of length $N_s = 4 \cdot M_1$, where $\mathbf{P}_u$ denotes a appropriate matrix containing $\mathrm{P}_u(k)$. The PN spreading does not effect the orthogonality of the transmission symbols:

$$\begin{aligned} \mathbf{h_i}^* \, \mathbf{h_j} &= (\mathbf{P}_u \, \mathbf{w_i})^* \, \mathbf{P}_u \, \mathbf{w_i} \\ &= \mathbf{w_i}^* \underbrace{\mathbf{P}_u^* \mathbf{P}_u}_{\text{ident. matrix}} \mathbf{w_i} \ = \ N_s \delta_{ij} \ . \end{aligned}$$

Now we perform a phase modulation of the real valued Walsh symbol, see lower branch in **Figure 1**. For this, the Walsh symbol is multiplied by a constant phase symbol $e^{j\varphi_k}$ which is determined by $\log_2(M_2)$ additional binary digits. When the channel consists of a complex multiplicative factor c (i.e. amplitude and phase shift) and additive noise $\mathbf{r}$, the received signal $\mathbf{s}$ turns out to be

$$\mathbf{s} = c e^{j\varphi_k} \mathbf{h_i} + \mathbf{r} \ .$$

At the receiver, the incoming signal is despread with the user specific PN sequence, see **Figure 2**. Then, the signal is correlated with all M_1 hypotheses of transmitted symbols $\mathbf{w_j}$ (discrete Hadamard transform, DHT). In our notation, the two steps simplify to the correlation with all possible symbols $\mathbf{h_j}$. With square law detection, we obtain for the M_1 correlations in each delay line of the RAKE receiver:

$$\begin{aligned} |\mathbf{h_j}^* \mathbf{s}|^2 &= |\mathbf{h_j}^* c \, e^{j\varphi_k} \mathbf{h_i} + \mathbf{h_j}^* \mathbf{r}|^2 \\ &= |\mathbf{h_j}^* c \, e^{j\varphi_k} \mathbf{h_i}|^2 + 2\mathrm{Re}\,\{r_1\} + |r_2|^2 \\ &= \underbrace{|e^{j\varphi_k}|^2}_{=1} \cdot |c \, N_s \delta_{ij}|^2 \ + \ \tilde{r} \quad . \end{aligned} \tag{1}$$

As can be seen from (1), the phase modulation does not effect the demodulation process for the Walsh symbols. The maximum likelihood receiver detects the value with maximum magnitude of the sum of the decision components given above. The index of this value (i_{max} in Figure 2) indicates the most likely transmitted symbol [2]. The additional data transmitted with $e^{j\varphi_k}$ is obtained by seperating the phase of the decided symbol or the phase difference of two consecutive symbols in the case of differential phase encoding, respectively.

The additional data transmitted per symbol can be used for *(i)* a *higher source data rate* with a slightly increased bit error rate, *(ii)* a *better error correction by improved channel coding*, or *(iii)* for any other purpose of interest (power control etc.).

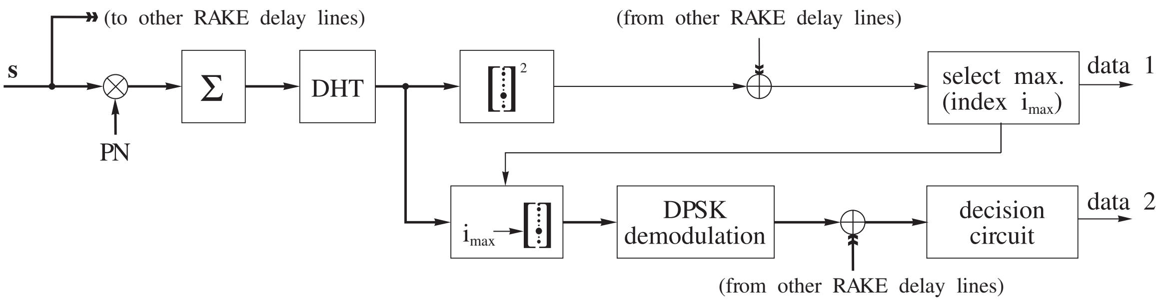

Figure 2: Noncoherent hybrid demodulation scheme (one RAKE branch)

3 Probability of Error for Hybrid Modulation

3.1 Probability of Error for AWGN channel

In this section, the channel is assumed to be an additive white Gaussian noise (AWGN) channel without memory, i.e. first of all, only one propagation path without fading is considered. For a general survey, we start with PSK instead of DPSK as the additional modulation type. As will be seen, it is convenient to derive the error probability for this coherent modulation type first and to derive the error probability for DPSK from it. In all cases, the phase modulation has been carried out using Gray encoding for the mapping of the binary digits to the PSK and DPSK symbols, respectively.

Due to the hybrid modulation, we have to distinguish two types of binary data: on the one hand, the $\log_2(M_1)$ bits belonging to each Walsh symbol and on the other hand, the $\log_2(M_2)$ bits belonging to each (D)PSK symbol. In the following, they will be called "Walsh-bits" and "(D)PSK-bits", respectively.

3.1.1 Hybrid Modulation using PSK

The analytical BER for the Walsh-bits for an AWGN channel is as follows. From the error probability of the Walsh symbols, which is [3]

$$P_W^{(AWGN)} = \sum_{n=1}^{M_1-1} \binom{M_1-1}{n} \frac{(-1)^{n+1}}{n+1}\, e^{-\frac{n}{n+1}\frac{E_S}{N_0}}, \tag{2}$$

(E_S/N_0 is the signal-to-noise ratio (SNR) of the Walsh symbols) the error probability of the corresponding Walsh-bits yields

$$P_{b,Walsh} = \frac{M_1/2}{M_1-1} \cdot P_W \ , \tag{3}$$

where the last equation holds for equiprobable orthogonal signals.

With (2), we obtain the probability of error for the bits of the M_2-PSK in the form

$$P_{b,PSK}^{(hybrid)} = \frac{1}{2}\, P_W + (1-P_W)\, P_{b,PSK}^{(M_2)}. \tag{4}$$

The first term follows from the fact that a false Walsh symbol detection still yields a correct PSK-symbol detection in $1/M_2$ of all cases, i.e. a *false* detection of the PSK-symbols occurs with probability $1-1/M_2$. Although (3) is originally valid for equiprobable orthogonal signals, the equation is applicable to the case considered here: if a false symbol is detected, all *phases* are equiprobable because the "symbol" consists of noise only – the Gray encoding is insignificant here. Hence, equivalent to (3), part of the corresponding binary symbols are nonetheless correct, which finally results in

$$\left(1-\frac{1}{M_2}\right) \cdot \frac{M_2/2}{M_2-1} = \frac{1}{2}. \tag{5}$$

The second term in eq. (4) takes into account the errors made even if the correct Walsh symbol decision is performed, which occurs with probability $(1-P_W)$. $P_{b,PSK}^{(M_2)}$ denotes the error probability of the M_2-PSK-bits which can be found in e.g. [2]. Here, for $M_2 \geq 8$, we used the approximation valid for Gray encoding [4]

$$P_{b,PSK}^{(M_2\geq 8)} \approx \frac{1}{\log_2(M_2)} \mathrm{erfc}\left(\sin\left(\frac{\pi}{M_2}\right)\sqrt{\frac{E_S}{N_0}}\right) \tag{6}$$

instead of the computationally expensive solution given in [2].

In **Figure 3**, the lower curve ("Walsh-bits") is obtained by evaluating (3), whereas the others result from (4). The circles stem from simulations and confirm the accuracy of the analytical results. It should be noted that the curve for the Walsh-bits superimposes the curves for the cases $M_2 = 2$ and $M_2 = 4$. The fact that the error probabilities for both 2-PSK and 4-PSK are obviously the same may be surprising. With hybrid modulation, the first term in (4), i.e the Walsh symbol error probability, predominates the total bit error probability whereas the M_2-dependent second term has no significant influence.

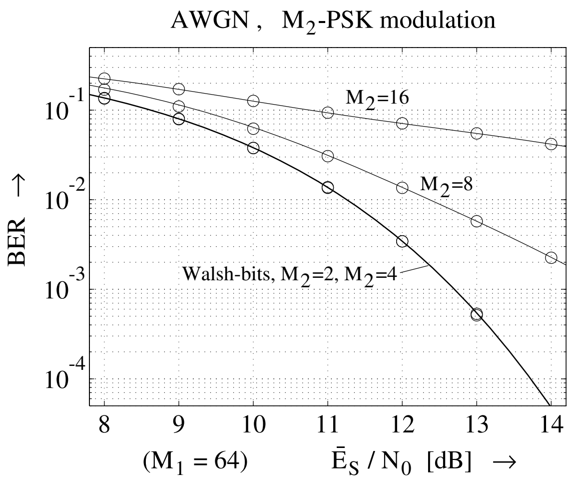

Figure 3: BER for hybrid modulation with PSK (analytical/simulation results, see text)

3.1.2 Hybrid Modulation using Differential PSK

In the following, we give the corresponding derivation for *differential* PSK. Of course, the use of a differential phase modulation has no effect on the error probability of the Walsh-bits (eq. (3)). However, the BER for the M_2-DPSK-bits changes significantly and turns out to be

$$P_{b,DPSK}^{(hybrid)} = P_W(1 - \frac{P_W}{2}) + (1 - P_W)^2 \, P_{b,DPSK}^{(M_2)} \, . \tag{7}$$

Let $\mathbf{w}_j(i)$ denote the Walsh symbol decision at instant i; due to the differential demodulation, we have to distinguish four cases in which a false DPSK symbol detection may occur:

a) $\mathbf{w}_j(i)$ false and $\mathbf{w}_j(i-1)$ false

b) $\mathbf{w}_j(i)$ false and $\mathbf{w}_j(i-1)$ correct

c) $\mathbf{w}_j(i)$ correct and $\mathbf{w}_j(i-1)$ false

d) $\mathbf{w}_j(i)$ correct and $\mathbf{w}_j(i-1)$ correct

On the assumption of statistically independent Walsh symbol detection, the probability of each joint event a)∼d) is simply the product of the probabilities of each single event. This is again $(1 - P_W)$ for a correct decision and P_W if a false decision is performed[3]. The cases a)∼c) together form the first term in (7):

$$\Big(\underbrace{P_W \cdot P_W}_{\text{a)}} + \underbrace{2 \cdot P_W\,(1 - P_W)}_{\text{b), c)}}\Big) \cdot \frac{1}{2}\,, \tag{8}$$

where the factor $1/2$ occurs according to equation (5).

If a correct Walsh symbol decision is made in *both* cases $\mathbf{w}_j(i)$ and $\mathbf{w}_j(i-1)$ (according to case d) or second term in (7)), a DPSK-bit error occurs nonetheless with probability

$$\underbrace{(1 - P_W) \cdot (1 - P_W)}_{\text{d)}} \cdot P_{b,DPSK}^{(M_2)} \, .$$

In the case $M_2 = 2$, $P_{b,DPSK}^{(M_2)}$ has to be calculated in the form [2]

$$P_{b,DPSK}^{(2)} = \frac{1}{2} \cdot e^{-E_S/N_0} . \tag{9}$$

For $M_2 = 4$, DPSK reveals a 2.3 dB loss compared to PSK, whereas for $M_2 \geq 8$ DPSK is approximately 3 dB poorer in performance [2]. Hence, we use (6) and correct the signal-to-noise ratio E_S/N_0 by 2.3 dB and 3.0 dB respectively, to obtain the error probability for M_2-DPSK.

Figure 4 again illustrates that the analytical results (solid lines) are in a good accordance with the simulation results ('∘'). It can be seen that the BER for the DPSK-bits is nearly twice as high in both cases $M_2 = 2$ and $M_2 = 4$ compared to the BER of the Walsh-bits. $M_2 \geq 8$ yields a considerably increased BER and therefore appears to be less appealing for applications where high transmission qualities are required.

[3]The probabilities of $\mathbf{w}_j(i)$ and $\mathbf{w}_j(i-1)$ are not distinguished because P_W is a mean probability.

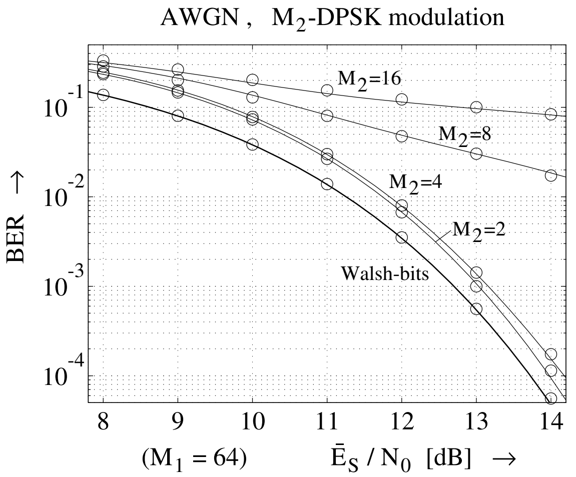

Figure 4: BER for hybrid modulation with DPSK (analytical/simulation results)

3.2 Probability of Error for Rayleigh Fading Channels

After having shown the BER performance for an AWGN channel, we now consider a mobile environment by introducing a fading channel with L propagation paths with equal mean energy and Rayleigh distributed amplitudes ("L-path Rayleigh channel"). Furthermore, we confine our attention to DPSK, only. This is because we want to keep the whole transmission scheme noncoherent.

In section 3.1.2, $M_2 = 4$ has been found to be a good choice for the degree of the additional differential phase modulation: the BER is only slightly increased compared to the case $M_2 = 2$, but twice the data can be transmitted with the DPSK symbols. $M_2 > 4$ reveals a significantly increased BER (see Figure 4) and is therefore not further investigated.

The derivation of the analytical error probability for hybrid DQPSK signals transmitted over L independently fading channels is unfortunately different to the derivation given in section 3.1.2 for AWGN channels. With Rayleigh fading, the assumption of statistically independent Walsh symbol detection does not hold any more. When the channel is in a deep fade, a false Walsh symbol detection is more likely compared to the case of a weak channel attenuation. For this, the simple derivation that leads to eq. (7) has to be raplaced by a more sophisticated one considering the statistics of the channel. Unfortunately, satisfying analytical results are not yet available.

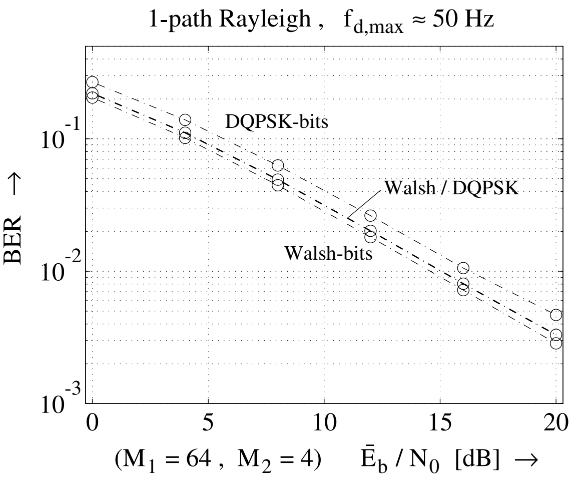

Figure 5: BER for hybrid modulation with DQPSK (simulation results)

Instead, we present the simulation results for transmission over a 1-path Rayleigh channel. In **Figure 5**, the different bit error rates for hybrid modulation are plotted versus the average received SNR per bit ($\bar{E_b}/N_0$). The lower curve shows the BER for the Walsh-bits, whereas the upper curve visualizes the BER for the DQPSK-bits. It should be noted that the bit error rate of the DQPSK-bits is *not* nearly doubled under fading conditions as it was in the case of AWGN (see Figure 4). The middle curve shows the overall BER resulting from averaging the two different bit error rates discussed above which is slightly higher compared to the Walsh-bit error rate. However, due to this modification the transmission rate can be increased by the factor $\log_2(M_1 \cdot M_2)/\log_2(M_1) = (6+2)/6 = 1.33$.

Figure 6 displays the bit error rates obtained by simulations ('$\circ$') assuming a 4-path Rayleigh channel. Here, the solid curves stem from the evaluation of eq. (7) although we have argued above that this is not the correct solution. With diversity, the probability that all signal components will fade simultaneously is reduced considerably. Hence, (7) can be seen as an approximation that holds for $L \gg 1$.

Note that the error probabilities P_W and $P_{b,DPSK}^{(M_2)}$ in eq. (7) have to be adapted for the L-path

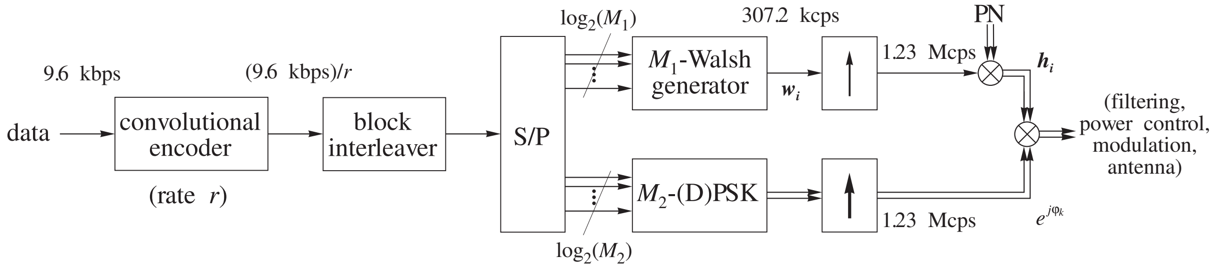

Figure 7: IS-95 extension: hybrid transmitter

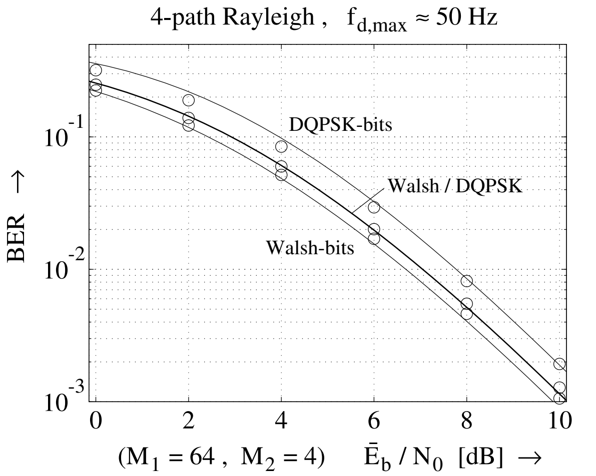

Figure 6: BER for hybrid modulation with DQPSK (analytical/simulation results)

Rayleigh fading channel, which is [2]:

$$P_W^{(L-Ray)} = 1 - \int_0^\infty \frac{x^{L-1}}{(L-1)!\,(1+\bar{\gamma}_c)^L} \cdot e^{-\frac{x}{1+\bar{\gamma}_c}} \left(1 - e^{-x} \sum_{k=0}^{L-1} \frac{x^k}{k!}\right)^{M_1-1}$$

and

$$P_{b,DPSK}^{(M_2=4)} = \frac{1}{2} - \frac{\mu/2}{\sqrt{2-\mu^2}} \sum_{k=0}^{L-1} \binom{2k}{k} \left(\frac{1-\mu^2}{4-2\mu^2}\right)^k$$

where $\bar{\gamma}_c$ is the average SNR per path of the Rayleigh channel and μ is defined as

$$\mu = \frac{\bar{\gamma}_c}{1+\bar{\gamma}_c} .$$

4 Summary

The concept developed here allows the transmission of additional data in a noncoherent CDMA communication system. **Figure 7** shows the application of the new hybrid scheme to the uplink of the IS-95 system. Here, the "additional" data stems from the same source as the data transmitted with the Walsh symbols. With this modification either the data rate can be decreased keeping the code rate r constant or the code rate can be increased without changing the source data rate. Further investigations will comprise the adaption of convolutional encoding and decoding for the hybrid concept presented here.

References

[1] A. Salmasi and K. Gilhousen. On the System Design Aspects of Code Division Multiple Access applied to Digital Cellular and Personal Communications Networks. In *Proc. IEEE Vehicular Technology Conference*, pages 57–62, May 1991.

[2] J.G. Proakis. *Digital Communications*. McGraw-Hill, third edition, 1995.

[3] M. Benthin. *Vergleich kohärenter und inkohärenter Codemultiplex-Übertragungskonzepte für zellulare Mobilfunksysteme*. PhD thesis, Dept. of Telecommunications, Hamburg University of Technology, Hamburg, Germany, March 1996.

[4] K.D. Kammeyer. *Nachrichtenübertragung*. Teubner, Stuttgart, 1992.

[5] K.S. Gilhousen, I.M. Jacobs, R. Padovani, A.J. Viterbi, L.A. Weaver Jr., and C.E. Wheatly III. On the Capacity of a Cellular CDMA System. *IEEE Trans. on Vehicular Technology*, 40(2):303–312, May 1991.